Force-in-domain GAN inversion

Guangjie Leng [1,*], **Yekun Zhu** [1,*], **Zhi-Qin John Xu** [1,2,†]

1 Institute of Natural Sciences and School of Mathematical Sciences and MOE-LSC, Shanghai Jiao Tong University
2 Qing Yuan Research Institute, Shanghai Jiao Tong University
lengguangjie@sjtu.edu.cn, zhuyekun123@sjtu.edu.cn, xuzhiqin@sjtu.edu.cn

Abstract

Empirical works suggest that various semantics emerge in the latent space of Generative Adversarial Networks (GANs) when being trained to generate images. To perform real image editing, it requires an accurate mapping from the real image to the latent space to leveraging these learned semantics, which is important yet difficult. An *in-domain* GAN inversion approach is recently proposed to constraint the inverted code within the latent space by forcing the reconstructed image obtained from the inverted code within the real image space. Empirically, we find that the inverted code by the *in-domain* GAN can deviate from the latent space significantly. To solve this problem, we propose a *force-in-domain* GAN based on the *in-domain* GAN, which utilizes a discriminator to force the inverted code within the latent space. The *force-in-domain* GAN can also be interpreted by a cycle-GAN with slight modification. Extensive experiments show that our *force-in-domain* GAN not only reconstructs the target image at the pixel level, but also align the inverted code with the latent space well for semantic editing.

Introduction

Generative Adversarial Networks (GANs) (Goodfellow et al. 2014) are successful in synthesizing high fidelity real images, such as face. A GAN consists of two key competing components, i.e., a generator part and a discriminator part. The generator network learns to map from a latent code, which is often sampled from a random distribution, to synthesized image. The discriminator network is trained to discriminate the real and the fake images, while the generator network is trained to make the synthesized image better to fool the discriminator.

A series of works (Goetschalckx et al. 2019; Jahanian, Chai, and Isola 2019; Shen et al. 2020) suggest that during the training, semantics spontaneously emerges within the latent code. The manipulation of the corresponding attributes of the latent code leads to change of the image in semantic. To enable the edit for real images, it is inevitable to obtain the inverted latent code for the real image. A simple minimization of the Mean Squared Error (MSE) between the generated samples and the associated real samples often leads to unsatisfied latent codes, because this approach

ignores the domain constraints for both inverted codes and reconstructed images. Small MSE does not imply the reconstructed images lying in the real image space. (Zhu et al. 2020) propose an *in-domain* GAN to force the reconstructed image lying in the real image space. The semantics editing based on the inverted code obtained by the *in-domain* GAN is much better than the naive approach. However, our experiments show that the inverted codes obtained by the *in-domain* GAN often deviate from the latent space significantly.

In this work, we further rescue in-domain crisis for the latent code. Based on the *in-domain* GAN, we propose a *force-in-domain* GAN. We add a discriminator network for the inverted code, therefore, the inversion network can be trained to be good enough to fool the discriminator. The *force-in-domain* GAN works between two domains, i.e., the real image domain and the latent code domain, thus, it can also be interpreted by a cycle-GAN but with slight modification. Our experiments show that the inverted code obtained by the *force-in-domain* GAN faithfully overlaps with latent space and reconstructs the target images at the pixel level and semantic level. In addition, extensive experiments show that our *force-in-domain* GAN shows good performance for semantic editing.

Related Works

Generative Adversarial Networks. GANs can learn the distribution of real images through adversarial training to generate realistic images (Goodfellow et al. 2014). It has been found that GANs spontaneously learn semantics in the latent space, which makes it feasible for controlling and explaining the generation process of GAN. In theory, (Chen et al. 2018; Arvanitidis, Hansen, and Hauberg 2017; Kuhnel et al. 2018) use Riemannian manifold to study the semantic editing of GANs, (Shen et al. 2020) focus on GANs that generates face images, and explores the connection between semantic space and actual images. However, due to the limitation of the GANs' structure, it is still difficult to freely edit the semantics of the latent space to change the generated images.

GAN Inversion. GANs learn a map from a random distribution to the real data distribution. Hence, it is for making inference on real images. GAN inversion can help us apply the semantic editing of the latent space to the generated

---

pictures. Given a fixed GAN model, GAN inversion aims at finding the most accurate latent code to recover the input images. The concept of GAN inversion is described in detail in (Perarnau et al. 2016; Lipton and Tripathi 2017; Creswell and Bharath 2018). Prior work to achieve GAN inversion are mainly divided into two ways, one is to set an optimization problem ((Abdal, Qin, and Wonka 2019; Ma, Ayaz, and Karaman 2019; Abdal, Qin, and Wonka 2020)), and the other is to use the trained GAN generator to construct the encoder ((Dumoulin et al. 2016; Donahue, Krähenbühl, and Darrell 2016; Zhu et al. 2019)).

Semantic Faces Editing with GANs. Semantic face editing aims to realize the manipulation of face attributes by manipulating the latent variables of the latent space. In semantic face editing, we hope that during the editing process, only the face attributes we operate have changed, while other face attributes remain unchanged. This is the difficulty and key point of semantic face editing. In order to achieve this goal, different methods are proposed: (Odena, Olah, and Shlens 2017; Chen et al. 2016; Tran, Yin, and Liu 2017) constructs a special loss function to realize the semantic editing of human faces; (Donahue et al. 2017; Shen et al. 2018) construct a special structure of GAN to achieve semantic editing.

Force-in-domain GAN inversion

In GAN model, the semantics refer to the emergent knowledge that GAN has learned from the observed data. Style-GAN model generates realistic images based on a disentangled representation in the latent space $\mathcal{W}$, which is obtained by samples from a Gaussian distribution through a fully-connected neural network (Karras, Laine, and Aila 2019). The latent space $\mathcal{W}$ is interpreted as a disentangled space of different image styles. A good GAN inversion model should not only recover input image by the pixel values, but also account for inverting the latent code semantically. For this purpose, we propose a *force-domain-guided* encoder which forces the inverted latent code having the same distribution with the latent space in StyleGAN. In general, the distribution of the latent space is unknown. To force the inverted latent code align with the original latent space, a new discriminator is added in our model, compared with the in-domain GAN (Zhu et al. 2020), as shown in Fig. 1.

Force-in-domain GAN structure

The *in-domain* GAN consists of the following components: encoder, $E(\cdot) : \mathcal{X} \to \mathcal{W}$, obtains the latent code corresponding to the input image; generator, $G(\cdot) : \mathcal{W} \to \mathcal{X}$, synthesizes high-quality images; discriminator $D(\cdot)$ distinguishes real data from synthesized data. Our *force-in-domain* GAN adds the following components: the fully connected layer FC from the StyleGAN that maps from the Gaussian distribution z to the latent space w^z; a new discriminator $D^w(\cdot)$ distinguishes inverted latent codes from real distribution of the latent space. Encoder E is the reverse mapping of the generator $G(\cdot)$, i.e., mapping from images $\mathbf{x}^{real}$ to latent code $\mathbf{w}$ that can recover the real images $\mathbf{x}^{real}$. Our purpose is to align w with w^z of the prior knowledge in the pre-trained StyleGAN model. The structure of the *force-in-domain* GAN is depicted in Fig. 1. Note that only green blocks are trainable.

Interpretation by Cycle-GAN

As shown in Fig. 2, cycle-GAN (without the red dashed block) transfers variables x in one domain to w in the other domain by E and also converts w back to x by G. In the context of *force-in-domain* GAN, two domains are the image domain and latent space, respectively. In Cycle-GAN, two discriminator networks are imposed to force $\hat{w}$ and $\hat{x}$ in their domains, respectively.

In our work, the generator G is already well-trained, and we only focus on the reconstruction of real images, therefore, *force-in-domain* GAN can be regarded as left part of cycle-GAN. In addition, a domain discriminator D (in the red dashed block) is equipped for the reconstructed image x' to ensure x' in the real image domain.
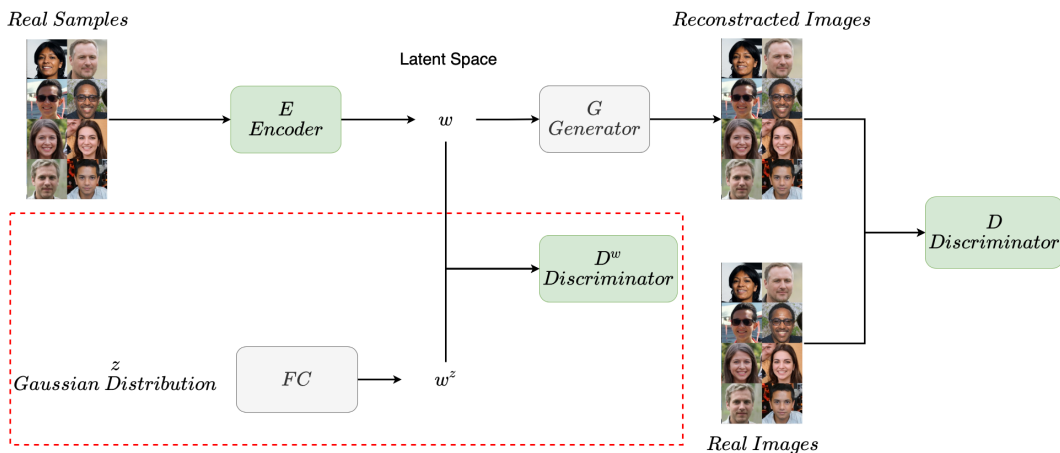

Figure 1: Our *force-in-domain* GAN inversion structure. Note that FC block is from the SyleGAN that maps from a Gaussian distribution to the latent space. Only green blocks are trainable.
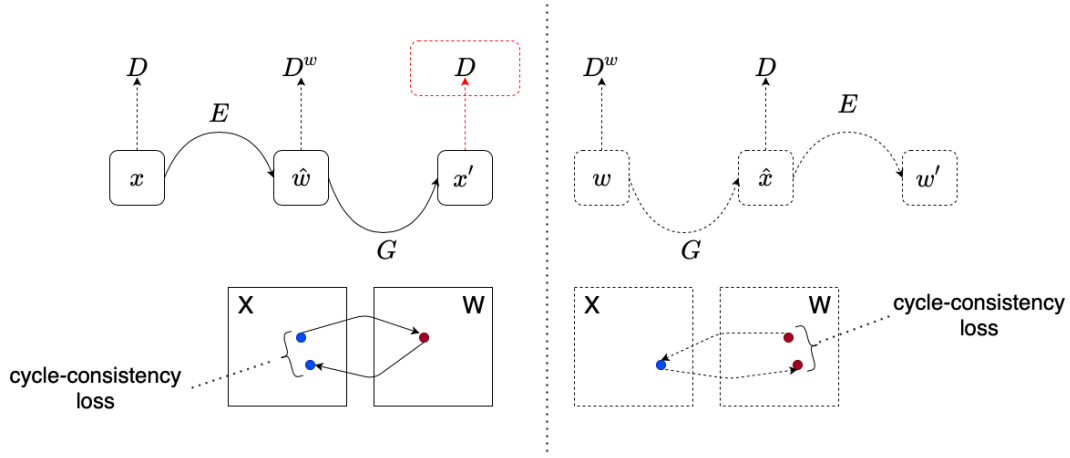
Figure 2: Interpretation by Cycle-GAN: the whole structure without the red block is the cycle-GAN. Our *force-in-domain* GAN is the left part with the red block and the block is the new discriminator we introduce in our network.

Adversarial Loss

We apply adversarial losses (Goodfellow et al. 2014) to the two discriminators. The objective is:

$$
\begin{aligned}
\mathcal{L}_{adv}^{D} = & \underset{\mathbf{x}^{real} \sim P_{data}}{\mathbb{E}} [\log(D(\mathbf{x}^{real}))] \\
& + \underset{\mathbf{x}^{real} \sim P_{data}}{\mathbb{E}} [\log(1 - D(G(E(\mathbf{x}^{real}))))] \quad (1) \\
& + \frac{\gamma}{2} \underset{\mathbf{x}^{real} \sim P_{data}}{\mathbb{E}} [\|\nabla_{\mathbf{w}} D(\mathbf{x}^{real})\|^2],
\end{aligned}
$$

$$
\begin{aligned}
\mathcal{L}_{adv}^{D^w} = & \underset{z \sim \mathcal{N}(0,\mathbf{I})}{\mathbb{E}} [\log(D^w(FC(z)))] \\
& + \underset{x^{real} \sim P_{data}}{\mathbb{E}} [log(1 - D_{\mathcal{W}}(E(x^{real})))] \quad (2) \\
& + \frac{\gamma}{2} \underset{w \sim FC(\mathcal{N}(0,\mathbf{I}))}{\mathbb{E}} [\|\nabla_{\mathbf{w}} D^w(w)\|^2],
\end{aligned}
$$

where γ is the hyper-parameter for the gradient regularization, P_{data} is the distribution of the real image data and $\mathcal{N}(0,\mathbf{I})$ denotes the Gaussian distribution.

Forward Cycle Consistent Loss

In GAN inversion tasks, it requires the reconstructed images close to the original images, i.e. $\mathbf{x} \to E(\mathbf{x}) \to G(E(\mathbf{x})) \approx \mathbf{x}$. This forward cycle consistent loss can be expressed as follows:

$$
\mathcal{L}_{cyc} = \underset{\mathbf{x}^{real} \sim P_{data}}{\mathbb{E}} \|\mathbf{x}^{real} - G(E(\mathbf{x}^{real}))\|_2. \quad (3)
$$

Perceptual Loss

Previous work has shown that high-quality images can be generated by defining and optimizing perceptual loss functions based on high-level features extracted from pre-trained networks (Johnson, Alahi, and Fei-Fei 2016). In our paper, we choose VGG (Simonyan and Zisserman 2014) as the pre-trained networks to introduce the perceptual loss:

$$
\mathcal{L}_{vgg} = \underset{\mathbf{x}^{real} \sim P_{data}}{\mathbb{E}} \|F(\mathbf{x}^{real}) - F(G(E(\mathbf{x}^{real})))\|_2, \quad (4)
$$

where F($\cdot$) denotes the VGG feature extraction model.

Force-in-domain Loss

We train the *force-in-domain* GAN, which is illustrated in Fig. 1, with the loss consisting of the forward cycle consistent loss, adversarial loss and the perceptual loss. By using these three kinds of losses, the encoder can inverse the input images to the latent space $\mathcal{W}$ and reconstruct the original image in both the pixel level and the semantic level.

$$
\mathcal{L}_{adv}^{E} = \mathcal{L}_{cyc} + \lambda_{adv}\mathcal{L}_{adv}^{D} + \lambda_{adv}^{D^w}\mathcal{L}_{adv}^{D^w} + \lambda_{vgg}\mathcal{L}_{vgg}, \quad (5)
$$

where λ's are hyper-parameters.

Experiments

In this section, we experimentally show that the latent codes obtained by the *force-in-domain* GAN inversion overlaps well with latent space of the original StyleGAN. We also utilize the *in-domain* GAN to edit real images.

Experimental settings

We conduct experiments on FFHQ dataset(Karras, Laine, and Aila 2019), which contains 70,000 high-quality face images. The generator G to be inverted is from the pre-trained StyleGAN (Karras, Laine, and Aila 2019). When training the *in-domain* GAN, the generator G and the FC components are fixed and we update the encoder E, the discriminator D and D^w. We set $\lambda_{vgg} = 5 \times e^{-5}$, $\lambda_{adv} = \lambda_{adv}^{D^w} = 0.1$ and $\gamma = 10$.

High quality of image reconstruction

Table 1: Quantitative Comparison between different inversion methods. For each model, we invert 10k images for evaluation. ↓ means lower is better.

Method	FID↓	MSE↓
In-Domain GAN Encoder without BN	17.55	0.49
Force-in-domain Encoder	15.06	0.067

A necessary condition for a good GAN inversion is that the reconstructed image is close to original image in both pixel and feature levels. To show that the *force-in-domain* GAN can faithfully reconstruct the original image, we quantitatively compute two common indexes, that is, Frchet Inception Distance (FID) (Heusel et al. 2017) and Mean-Square Error (MSE). The FID is a metric for assessing the quality of images generated by GAN, which compares the distribution of generated images with the distribution of real images that were used to train the generator. MSE quantifies the difference between the reconstructed images and the original images in the pixel level. We randomly select 10,000 images from FFHQ dataset for computation. As shown in Table 1, both FID and MSE of the *force-in-domain* GAN are much smaller that those of *in-domain* GAN. Therefore, the *force-in-domain* GAN can improve the fidelity of the image reconstruction. Next, we would show in the latent space, the *force-in-domain* GAN can also align the inverted latent codes well with the original latent space, thus, serving as a good model for real images editing due to the preservation of the semantics in latent space.

Image inversion

We found that in the process of image reconstruction, *in-domain* GAN would produce some strange images shown in Fig. 3. For these images, our *force-in-domain* GAN can reconstruct well. Note that in our experiments, *force-in-domain* GAN never produce such strange images. (Zhu et al. 2020) proposed BN-*in-domain* GAN recently to solve this problem, but our further projection results also show that the reconstructed latent code in BN-*in-domain* GAN is not on its real manifold, either.

Figure 3: Reconstruction of images from FFHQ. Images in the left are the original. Images in the middle are the reconstruction results of *in-domain* GAN. Images in the right are the reconstruction results of *force-in-domian* FA

Good alignment of latent codes

It is reasonable that the high quality of image reconstruction is due to the good inverted latent codes. Compared with the *in-domain* GAN, the *force-in-domain* GAN makes the inverted latent code closer to the original latent space in the

sense of distribution. To verify this point, we project high-dimensional latent codes into two-dimensional space. The procedure to perform this comparison is depicted in Fig. 4. The original latent code w^z is obtained through the sampling from Gaussian distribution and the FC component. We pass w^z through generator G to obtain a image and then use the encoder E to obtain the inverted latent code w. Then, we project a bunch of w^z's and w's into two-dimensional space by two methods, i.e., principle component analysis (PCA) and t-SNE (Van der Maaten and Hinton 2008). For both methods, we sample $100,000$ samples from the Gaussian distribution to ensure enough precision.
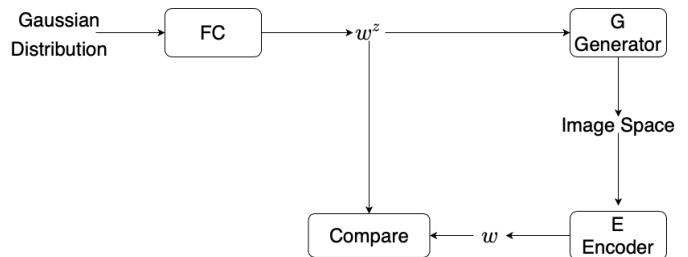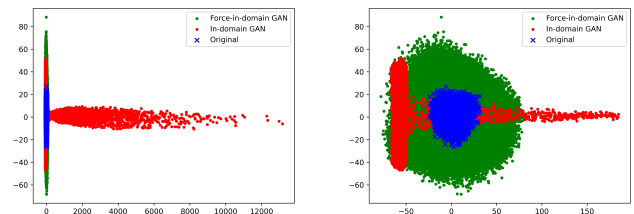

Figure 4: The idea of our projection method

The projection results of PCA method are shown in Fig. 5(a). There are so many outliers of the *in-domain* GAN that we cannot visualize the comparison clearly. For visualization, we remove part of the data of *in-domain* GAN, whose absolute values are bigger than ten times of the original projection results. As shown in Fig. 5(b), the projection of the inverted latent codes of *in-domain* GAN deviate significantly from the true distribution, and there are many outliers that are far away from the true distribution. The projection results of *force-in-domain* GAN are relatively concentrated and can cover the true distribution.
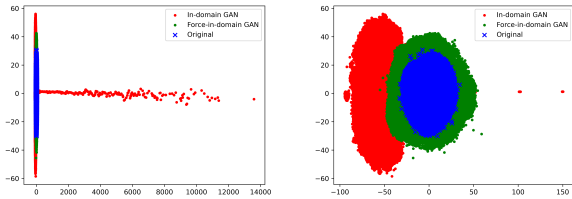

(a) Original projection results   (b) Projection results without outliers

Figure 5: Projection results using PCA method. In both figures, "Original" can the projection results of the true distribution of the latent codes (sampling from Gaussian distribution and mapping to the space); "*Force-in-domain* GAN" means the projection results of *force in-domain* GAN and "In-domain GAN" means the projection results of *in-domain* GAN. Further more, both of the results of force-in-domian GAN and in-domain GAN are derived by the same samples.

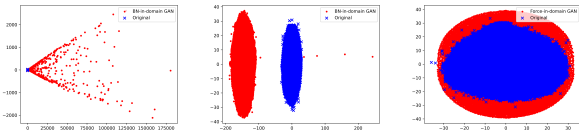For the projection results of t-SNE method, as shown in

Fig. 6(a), the projection of the *in-domain* GAN also has many outliers. We similarly remove outliers and as shown in Fig. 6(b), the projection of the *in-domain* GAN is significantly different from the projection of original latent codes. However, the projection of the *force-in-domain* GAN overlaps with the projection of original latent codes much better. While preparing this paper, (Zhu et al. 2020) release a

(a) Original projection results (b) Projection results without outliers

Figure 6: Projection results using t-SNE method. Illustration is the same as Fig. 5.

better *in-domain* GAN by adding batch normalization. For convenience, we denote this model by *BN-in-domain* GAN. We perform similar projection examination for this *BN-in-domain* GAN. Since the FC components in *BN-in-domain* GAN and *force-in-domain* GAN are different, the original latent codes of these two models are different for a same Gaussian sample. We display the comparison of the inverted codes and the original latent codes for the *BN-in-domain* GAN in Fig. 7(a,b) and for the *force-in-domain* GAN in Fig. 7(c), respectively. Similarly, the inverted codes of the *force-in-domain* GAN align well with the original latent codes while the *BN-in-domain* GAN fails to align the inverted latent codes with the original latent space. From the projection

(a) Original projection results (b) Projection results without outliers (c) Original projection results of our model

Figure 7: Projection results using t-SNE method for *BN-in-domain* GAN in (a,b) and *force-in-domain* GAN in (c). Illustration is the similar as Fig. 5.

results, we can find that our method can force the encoder to map real images much closer to the true latent space, thus, explaining the well reconstruction of image and being a better model for semantics editing for real images.

Real Image Editing

In this section, we apply *force-in-domain* GAN inversion approach in real image editing tasks, including image interpo-
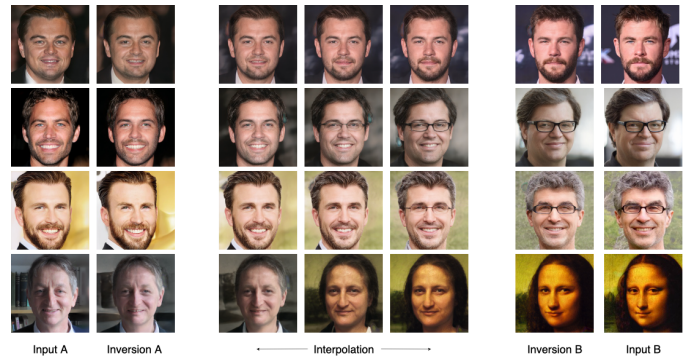

Figure 8: Image interpolation results using our *force-in-domian* GAN.

lation, semantic diffusion and semantic manipulation.

Image Interpolation For given two images, we can interpolate them similar to the interpolation between two points. Image interpolation aims at semantically interpolating two images but not simply on the pixel level. Thus, it is appropriate to interpolate two images through their latent codes. It is reasonably to expect that the semantic of the interpolated image would vary continuously with the weights of two inverted codes. As shown in Fig. 8, for the two input images (first and the last column), we use *force-in-domain* GAN to obtain the inversion images. Then, we interpolate the inverted latent codes and feed the interpolated latent codes into the generator. A smooth variation of the interpolated images can be clearly achieved by the *force-in-domain* GAN.
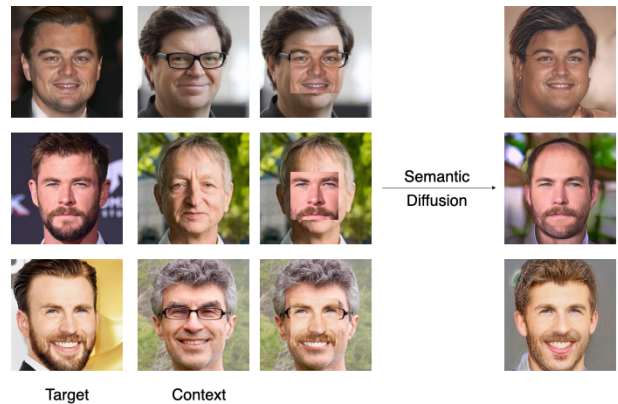

Figure 9: Semantic diffusion result using our *force-in-domain* GAN.

Semantic Diffusion. Semantic diffusion is a task that diffuses a representative part of the target image into the context of another image. In our task, we diffuse the center part of a face image to another face image. As shown in Fig. 9, we mask the context face (second column) by the center of the target face (first column). We obtain the inverted latent code of the mixed face through *force-in-domain* GAN and reconstruct the mixed face through the generator. As shown in the last column, the reconstructed faces well preserve the identity of the target fact and reasonably integrate into dif-

ferent surroundings.

Semantic Manipulation. An important and interesting task for GAN inversion is image manipulation in semantic level. As the latent code encodes rich semantic knowledge during the training, it is able to find decision boundaries for different semantic attributes, by which we can manipulate the image through tuning the latent code towards or away from the boundary. Following the procedure in (Shen et al. 2020), we first use a pre-trained attribute prediction model [1] to assign attribute scores for synthesized images. Then, for each attribute, we learn a linear SVM, resulting in a decision boundary. Then the image editing process can be formulated as

$$\mathbf{x}^{edit} = G(\mathbf{z}^{inv} + \alpha \mathbf{n}),$$

where $\mathbf{n}$ is the normal direction of the decision boundary for a particular semantic attribute and α is the step size for manipulation. It is also expected to see a continuous variation of the edited image as the step size α. As shown in Fig. 10, we manipulate real images on the semantics of smile, age, pose and glass based on the *force-in-domain* GAN inversion. For different examples, we obtain satisfying manipulation results.

Conclusion

A key factor that affects the quality of GAN inversion is whether the inverted code lies in the original latent space. In this work, we have proposed a *force-in-domain* GAN that can faithfully align the inverted codes with original latent space, thus, being a good model for real image editing.

---

[1]https://www.faceplusplus.com.cn

References

Abdal, R.; Qin, Y.; and Wonka, P. 2019. Image2stylegan: How to embed images into the stylegan latent space? In *Proceedings of the IEEE/CVF International Conference on Computer Vision*, 4432–4441.

Abdal, R.; Qin, Y.; and Wonka, P. 2020. Image2stylegan++: How to edit the embedded images? In *Proceedings of the IEEE/CVF Conference on Computer Vision and Pattern Recognition*, 8296–8305.

Arvanitidis, G.; Hansen, L. K.; and Hauberg, S. 2017. Latent space oddity: on the curvature of deep generative models. *arXiv preprint arXiv:1710.11379* .

Chen, N.; Klushyn, A.; Kurle, R.; Jiang, X.; Bayer, J.; and Smagt, P. 2018. Metrics for deep generative models. In *International Conference on Artificial Intelligence and Statistics*, 1540–1550. PMLR.

Chen, X.; Duan, Y.; Houthooft, R.; Schulman, J.; Sutskever, I.; and Abbeel, P. 2016. Infogan: Interpretable representation learning by information maximizing generative adversarial nets. *arXiv preprint arXiv:1606.03657* .

Creswell, A.; and Bharath, A. A. 2018. Inverting the generator of a generative adversarial network. *IEEE transactions on neural networks and learning systems* 30(7): 1967–1974.

Donahue, C.; Lipton, Z. C.; Balsubramani, A.; and McAuley, J. 2017. Semantically decomposing the latent

Figure 10: Semantic manipulation result using our *force-in-domain* GAN.

spaces of generative adversarial networks. *arXiv preprint arXiv:1705.07904* .

Donahue, J.; Krähenbühl, P.; and Darrell, T. 2016. Adversarial feature learning. *arXiv preprint arXiv:1605.09782* .

Dumoulin, V.; Belghazi, I.; Poole, B.; Mastropietro, O.; Lamb, A.; Arjovsky, M.; and Courville, A. 2016. Adversarially learned inference. *arXiv preprint arXiv:1606.00704* .

Goetschalckx, L.; Andonian, A.; Oliva, A.; and Isola, P. 2019. Ganalyze: Toward visual definitions of cognitive image properties. In *Proceedings of the IEEE/CVF International Conference on Computer Vision*, 5744–5753.

Goodfellow, I. J.; Pouget-Abadie, J.; Mirza, M.; Xu, B.; Warde-Farley, D.; Ozair, S.; Courville, A.; and Bengio, Y. 2014. Generative adversarial networks. *arXiv preprint arXiv:1406.2661* .

Heusel, M.; Ramsauer, H.; Unterthiner, T.; Nessler, B.; Klambauer, G.; and Hochreiter, S. 2017. GANs Trained by a Two Time-Scale Update Rule Converge to a Nash Equilibrium. .

Jahanian, A.; Chai, L.; and Isola, P. 2019. On the" steerability" of generative adversarial networks. *arXiv preprint arXiv:1907.07171* .

Johnson, J.; Alahi, A.; and Fei-Fei, L. 2016. Perceptual losses for real-time style transfer and super-resolution. In *European conference on computer vision*, 694–711. Springer.

Karras, T.; Laine, S.; and Aila, T. 2019. A style-based generator architecture for generative adversarial networks. In *Proceedings of the IEEE/CVF Conference on Computer Vision and Pattern Recognition*, 4401–4410.

Kuhnel, L.; Fletcher, T.; Joshi, S.; and Sommer, S. 2018. Latent space non-linear statistics. *arXiv preprint arXiv:1805.07632* .

Lipton, Z. C.; and Tripathi, S. 2017. Precise recovery of latent vectors from generative adversarial networks. *arXiv preprint arXiv:1702.04782* .

Ma, F.; Ayaz, U.; and Karaman, S. 2019. Invertibility of convolutional generative networks from partial measurements .

Odena, A.; Olah, C.; and Shlens, J. 2017. Conditional image synthesis with auxiliary classifier gans. In *International conference on machine learning*, 2642–2651. PMLR.

Perarnau, G.; Van De Weijer, J.; Raducanu, B.; and Álvarez, J. M. 2016. Invertible conditional gans for image editing. *arXiv preprint arXiv:1611.06355* .

Shen, Y.; Luo, P.; Yan, J.; Wang, X.; and Tang, X. 2018. Faceid-gan: Learning a symmetry three-player gan for identity-preserving face synthesis. In *Proceedings of the IEEE conference on computer vision and pattern recognition*, 821–830.

Shen, Y.; Yang, C.; Tang, X.; and Zhou, B. 2020. Interfacegan: Interpreting the disentangled face representation learned by gans. *IEEE Transactions on Pattern Analysis and Machine Intelligence* .

Simonyan, K.; and Zisserman, A. 2014. Very deep convolutional networks for large-scale image recognition. *arXiv preprint arXiv:1409.1556* .

Tran, L.; Yin, X.; and Liu, X. 2017. Disentangled representation learning gan for pose-invariant face recognition. In *Proceedings of the IEEE conference on computer vision and pattern recognition*, 1415–1424.

Van der Maaten, L.; and Hinton, G. 2008. Visualizing data using t-SNE. *Journal of machine learning research* 9(11).

Zhu, J.; Shen, Y.; Zhao, D.; and Zhou, B. 2020. In-domain gan inversion for real image editing. In *European Conference on Computer Vision*, 592–608. Springer.

Zhu, J.; Zhao, D.; Zhou, B.; and Zhang, B. 2019. Lia: Latently invertible autoencoder with adversarial learning .